Supplementary Information (SI) for Physical Chemistry Chemical Physics.

Supporting Information:
Common mechanism of dual emission in linearly-linked donor-acceptor-type thermally activated delayed fluorescence molecules

Tomohiro Ryu[1], Arvydas Ruseckas[2], Masaki Saigo[1], Kiyoshi Miyata[1],
Youichi Tsuchiya[3], Hajime Nakanotani[3], Chihaya Adachi[3],
Ifor D. W. Samuel[2], Ken Onda[1]*

[1]Department of Chemistry, Faculty of Science, Kyushu University
744 Motooka, Nishi, Fukuoka 819-0395, Japan
[2]Organic Semiconductor Centre, School of Physics and Astronomy, University of St Andrews
North Haugh, St Andrews Fife, KY16 9SS, UK
[3]Center for Organic Photonics and Electronics Research, Kyushu University
744 Motooka, Nishi, Fukuoka 819-0395, Japan

**E-mail* *konda@chem.kyushu-univ.jp*

Contents

SI-1. Emission properties

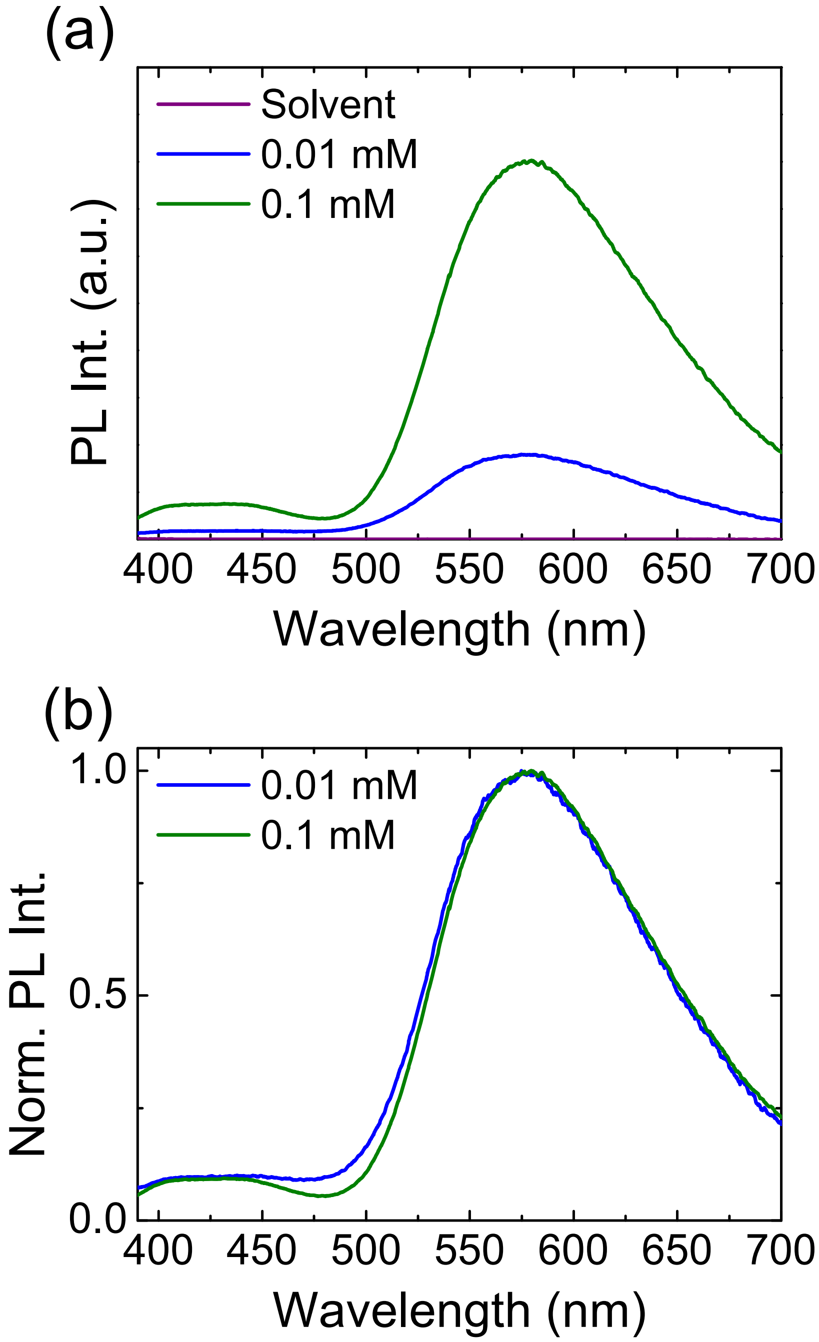

Figure S1. Concentration-dependent steady-state spectra of PTZ-TRZ in 0.01 mM (blue) and 0.1 mM (green) toluene solutions. (a) Comparison between spectra of solvent (toluene, purple) and PTZ-TRZ, (b) Normalized PL spectra of PTZ-TRZ in toluene solution. In all measurements, the excitation wavelength was 345 nm.

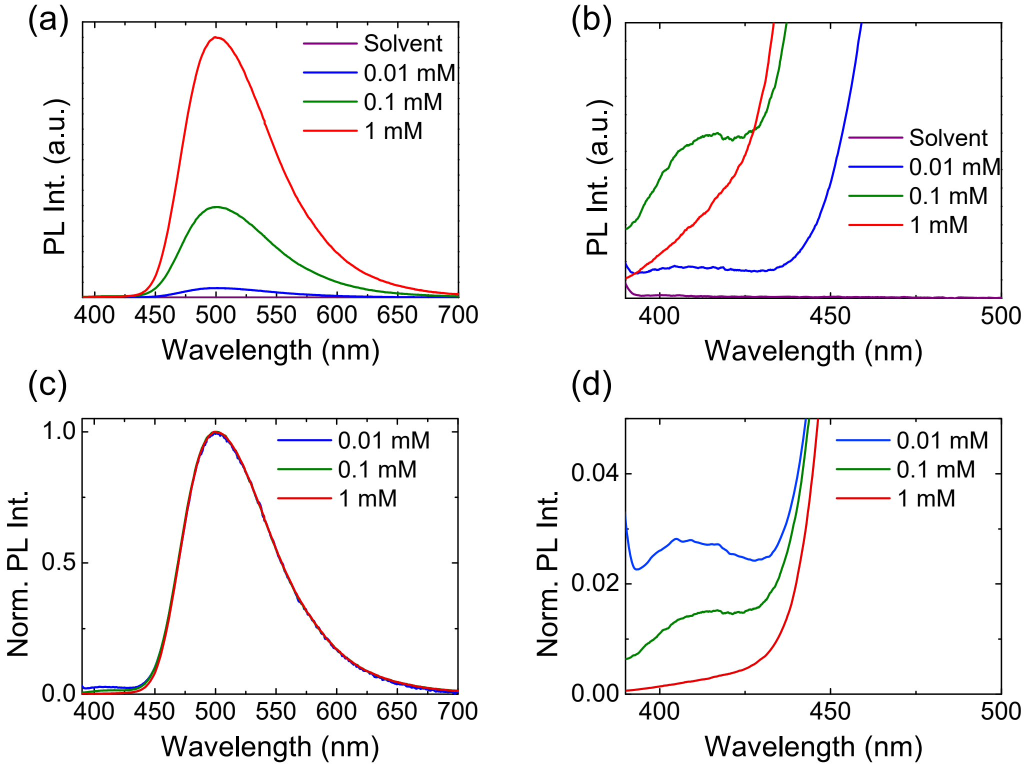

Figure S2. Concentration-dependent steady-state spectra of DMAC-TRZ in 0.01 mM (blue), 0.1 mM (green), and 1 mM (red) toluene solutions. (a) Comparison between spectra of solvent (toluene, purple) and PTZ-TRZ, (b) Expanded steady-state PL spectra in the range of 360 - 500 nm. (c) Normalized PL spectra of DMAC-TRZ in toluene solution and (c) Expanded steady-state PL spectra in the range of 360 - 500 nm. In all measurements, the excitation wavelength was 345 nm.

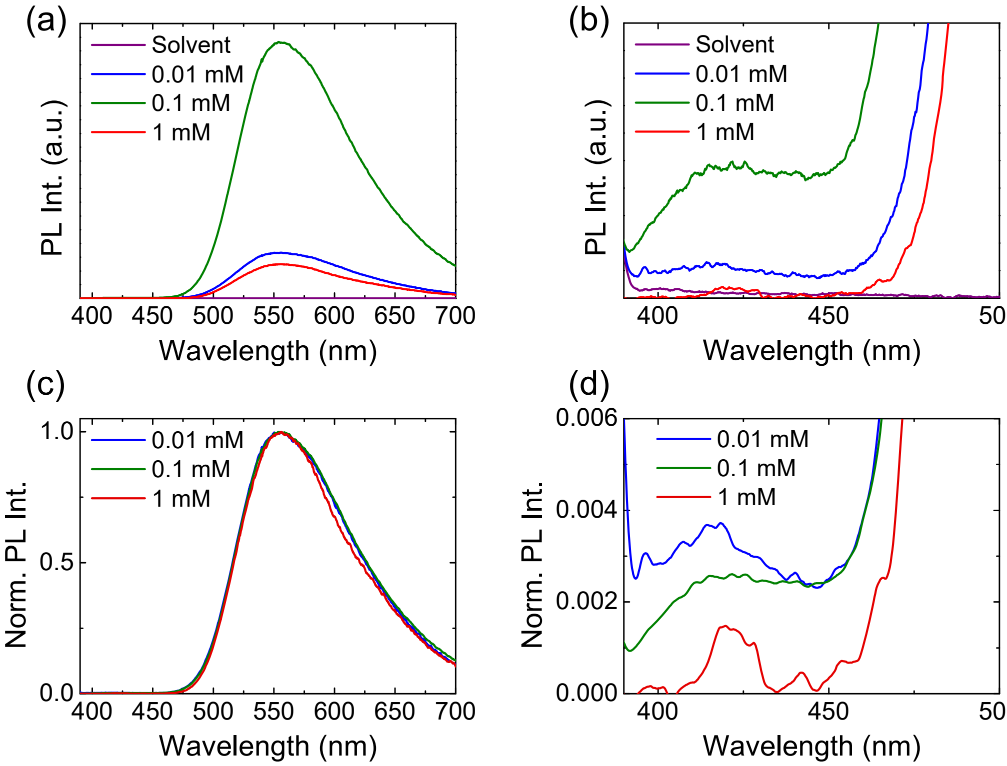

Figure S3. Concentration-dependent steady-state spectra of PXZ-TRZ in 0.01 mM (blue), 0.1 mM (green), and 1 mM (red) toluene solutions. (a) Comparison between spectra of solvent (toluene, purple) and PTZ-TRZ, (b) Expanded steady-state PL spectra in the range of 360 - 500 nm. (c) Normalized PL spectra of PXZ-TRZ in toluene solution and (c) Expanded steady-state PL spectra in the range of 360 - 500 nm. In all measurements, the excitation wavelength was 345 nm.

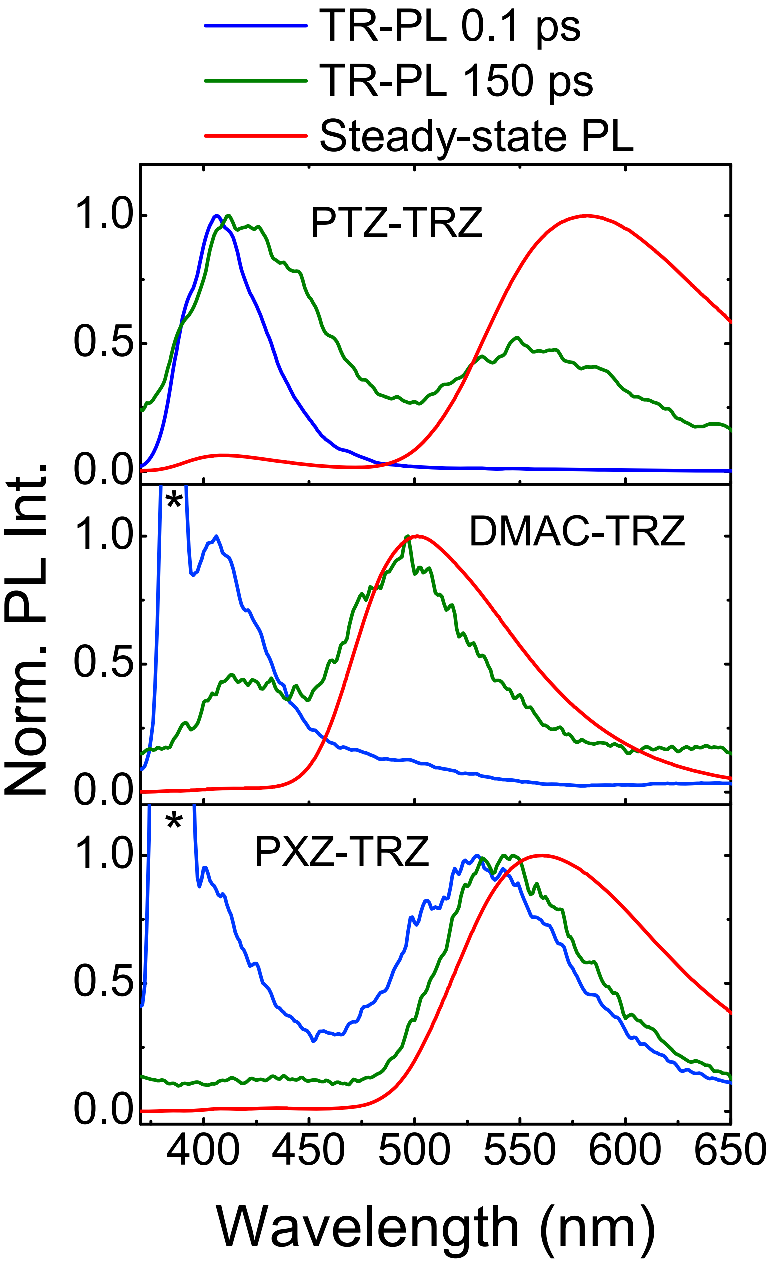

Figure S4. Comparison of normalized TR-PL spectra at 0.1 ps and 150 ps and normalized steady-state PL spectra for PTZ-TRZ, DMAC-TRZ, and PXZ-TRZ.

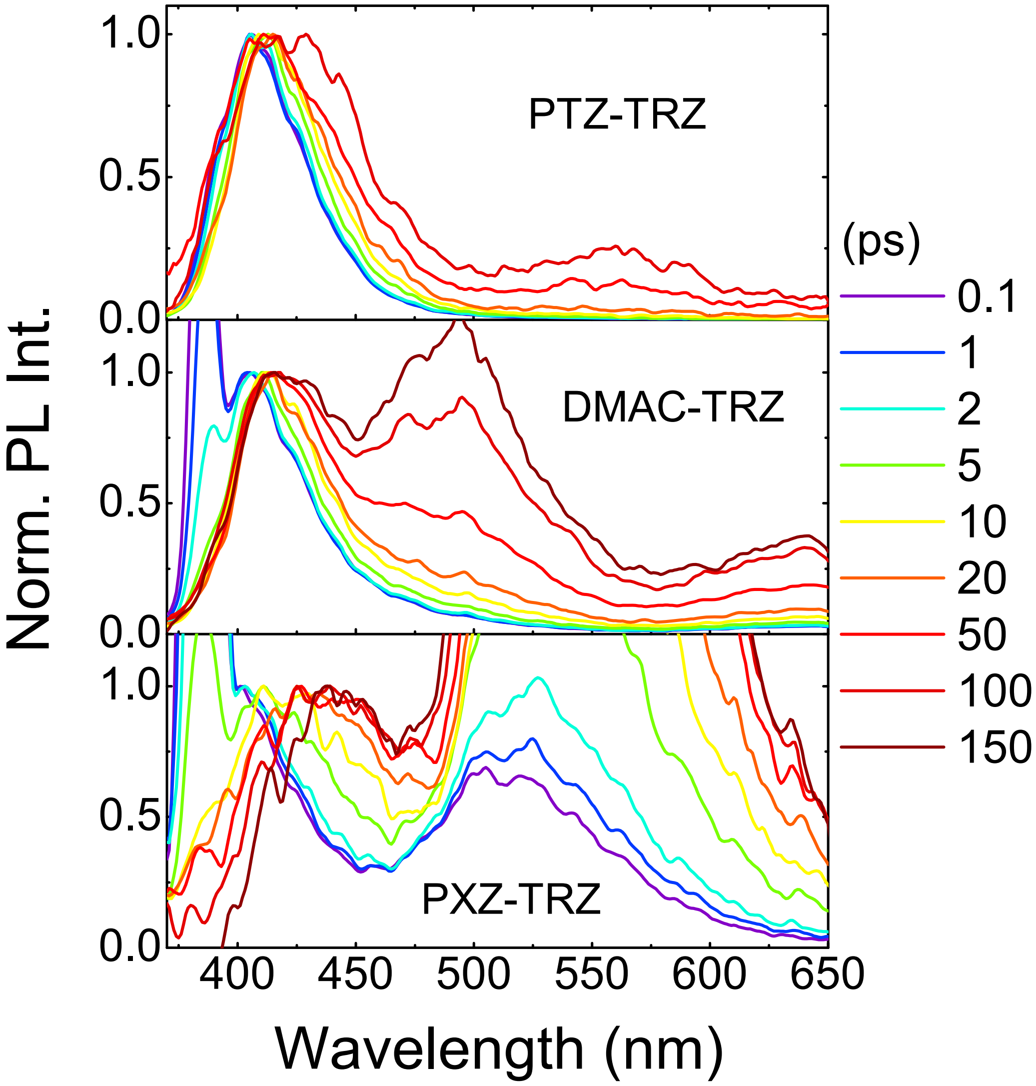

Figure S5. The normalized TR-PL spectra in PTZ-TRZ, DMAC-TRZ, and PXZ-TRZ.

SI-2. Energies and oscillator strengths estimated by quantum chemical calculations

Table S1. The calculated oscillator strength (*f*) of each state in each conformer of each molecule. All values were calculated with the optimized structure of the S_0 state (the upper part) and S_1 state (the lower part), respectively.

f **(S_0 state)**		**S_1**	**S_2**	**S_3**	**S_4**	**S_5**
PTZ-TRZ	q-copl.	<0.01	0.91	0.12	<0.01	<0.01
	perp.	<0.01	0	<0.01	0	0
DMAC-TRZ	q-copl.	0	0.97	0	<0.01	0.00
	perp.	<0.01	0	<0.01	0	0
PXZ-TRZ	q-copl.	<0.01	0.84	0.00	<0.01	<0.01
	perp.	<0.01	0	<0.01	<0.01	0

f **(S_1 state)**		**S_1**	**S_2**	**S_3**	**S_4**	**S_5**
PTZ-TRZ	q-copl.	0	0.74	<0.01	0	<0.01
	perp.	0	0	<0.01	0	0
DMAC-TRZ	q-copl.	0	0.78	0	0.10	0.25
	perp.	0	0	<0.01	<0.01	0
PXZ-TRZ	q-copl.	0	0.67	<0.01	<0.01	0.21
	perp.	0	0	<0.01	<0.01	0

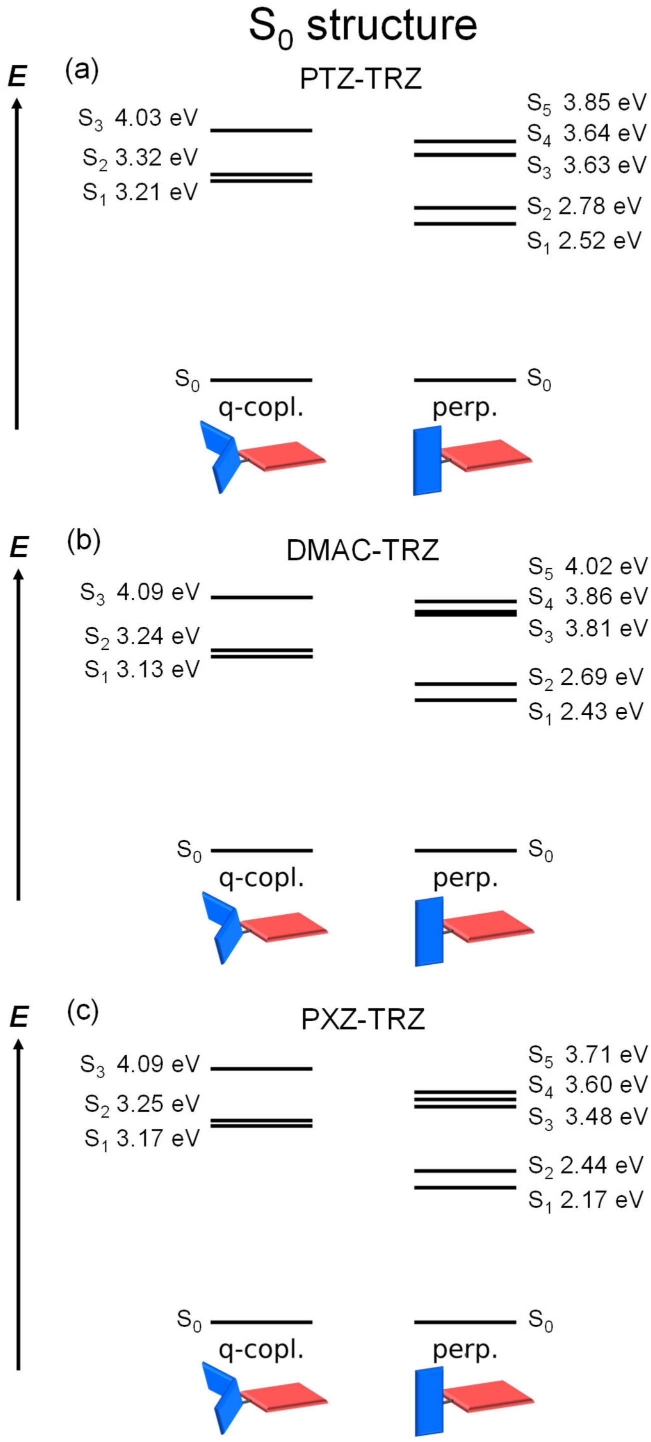

Figure S6. The calculated energies of the S_1 to S_3 states in the q-copl. conformer and the S_1 to S_5 states in the perp. conformer. All the values were calculated with the optimized structure of the S_0 state and based on time-dependent (TD)-DFT.

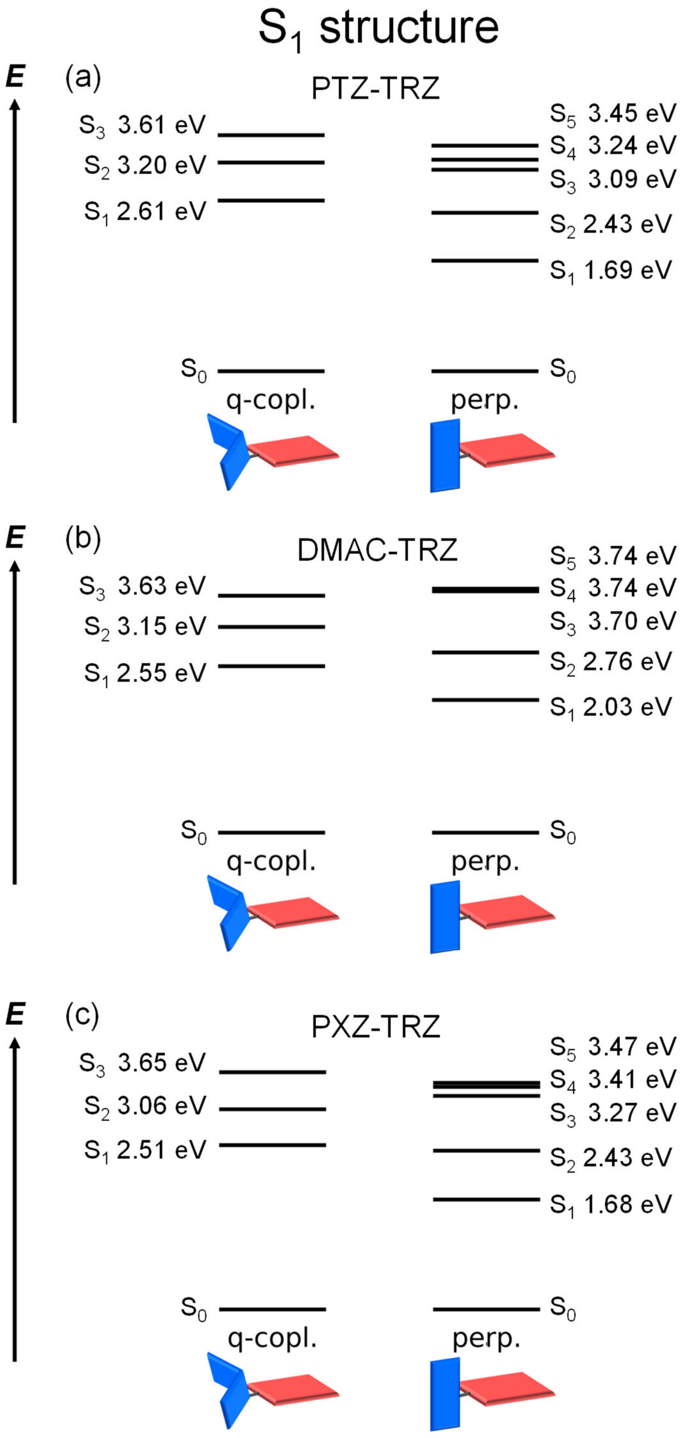

Figure S7. The calculated energies of the S_1 to S_3 states in the q-copl. conformer and the S_1 to S_5 state in the perp. conformer. All the values were calculated with the optimized structure of the S_1 state and based on time-dependent (TD)-DFT.

SI-3. Natural transition orbitals (NTOs)

Quantum chemical calculations were performed using *Gaussian 16 C.01* package.[1] The hole and electron of q-copl. and perp. conformers of the PTZ-TRZ, PXZ-TRZ, and PXZ-TRZ were calculated based on TD-DFT. The solvent effect was examined by using the polarizable continuum model of toluene solution (dielectric constant: 2.38). The calculations were conducted with the S_1 to S_5 state with the structure fixed in the S_1 state of these molecules.

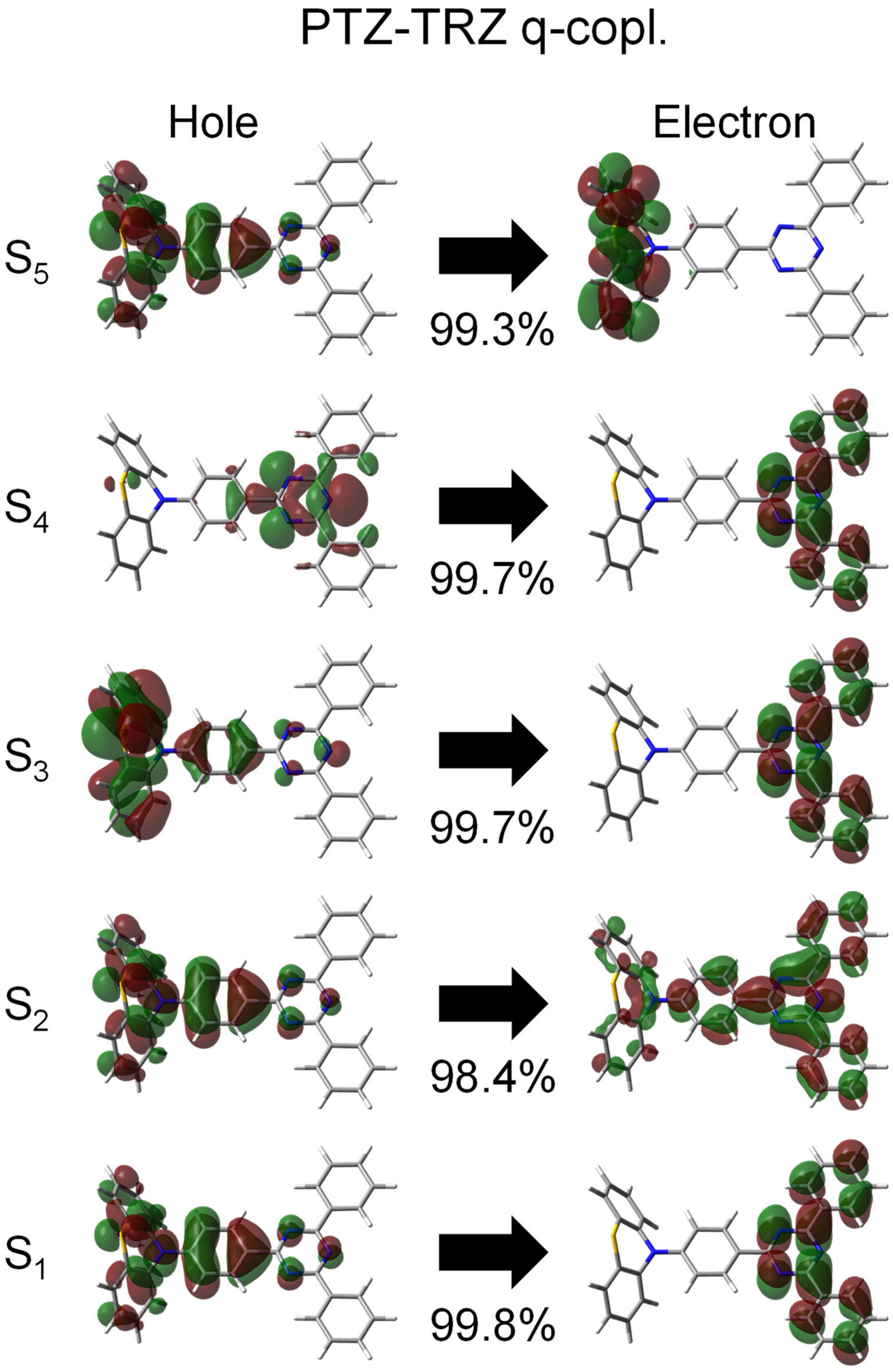

Figure S8. The NTOs of the q-copl. conformer of PTZ-TRZ in the S_1 to S_5 state.

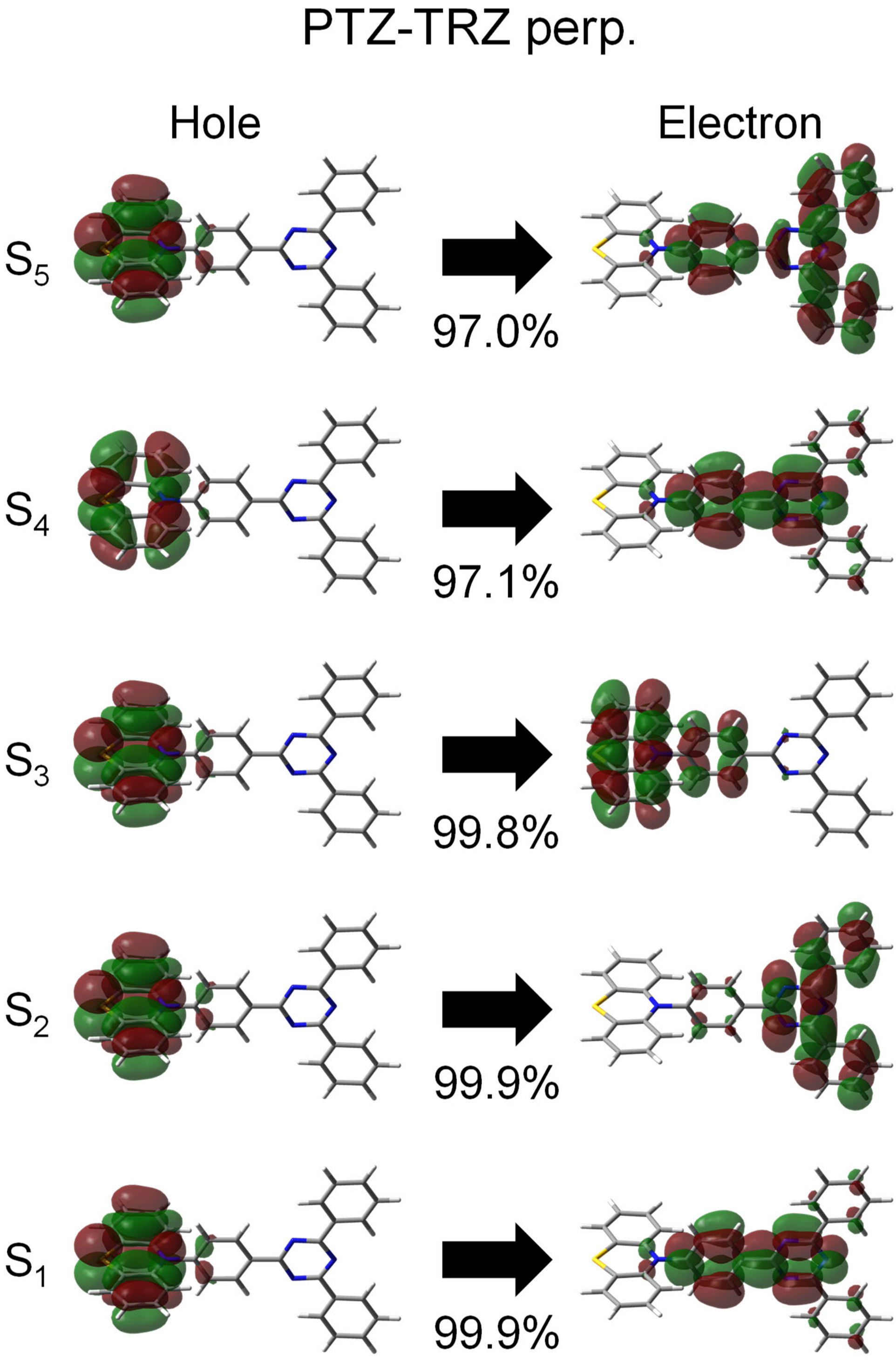

Figure S9. The NTOs of the perp. conformer of PTZ-TRZ in the S_1 to S_5 state.

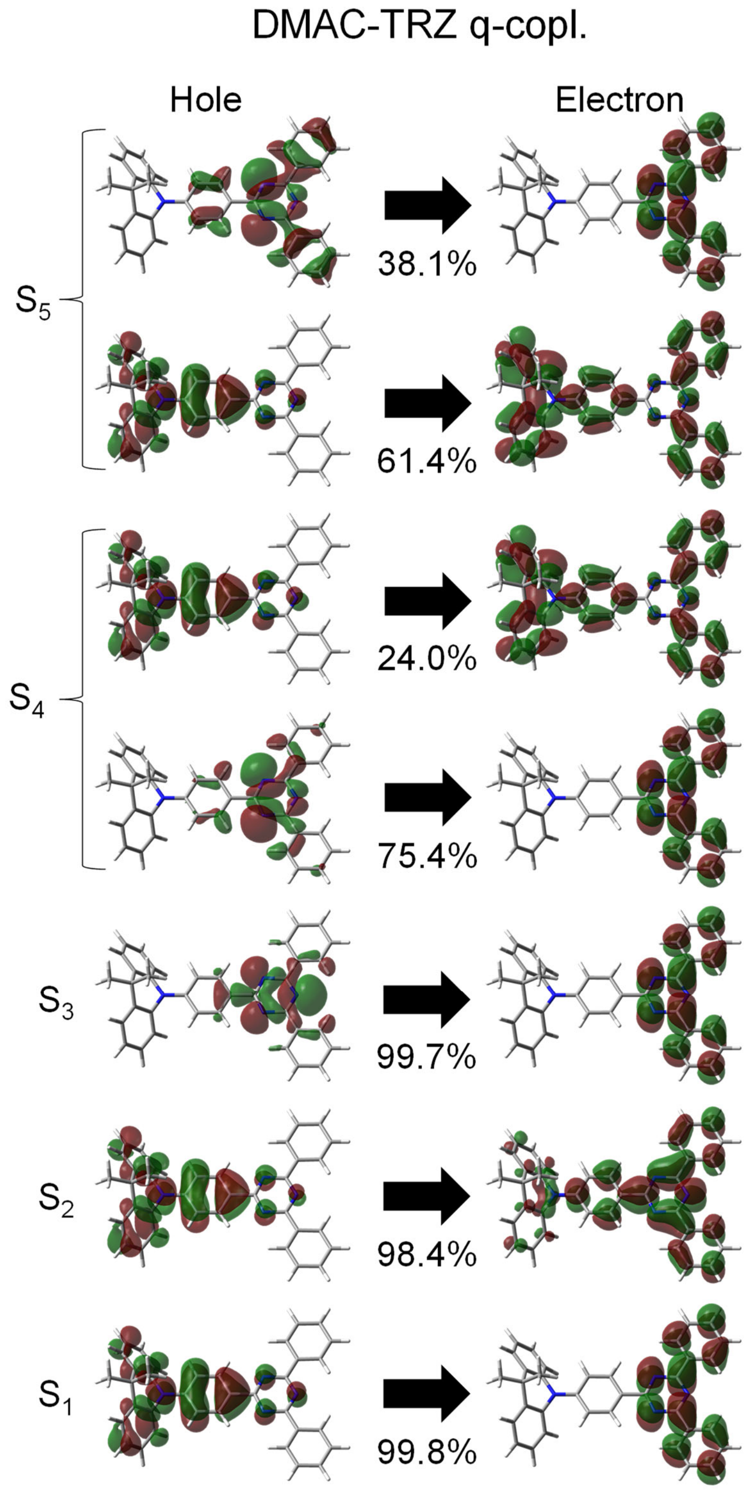

Figure S10. The NTOs of the q-copl. conformer of DMAC-TRZ in the S_1 to S_5 state.

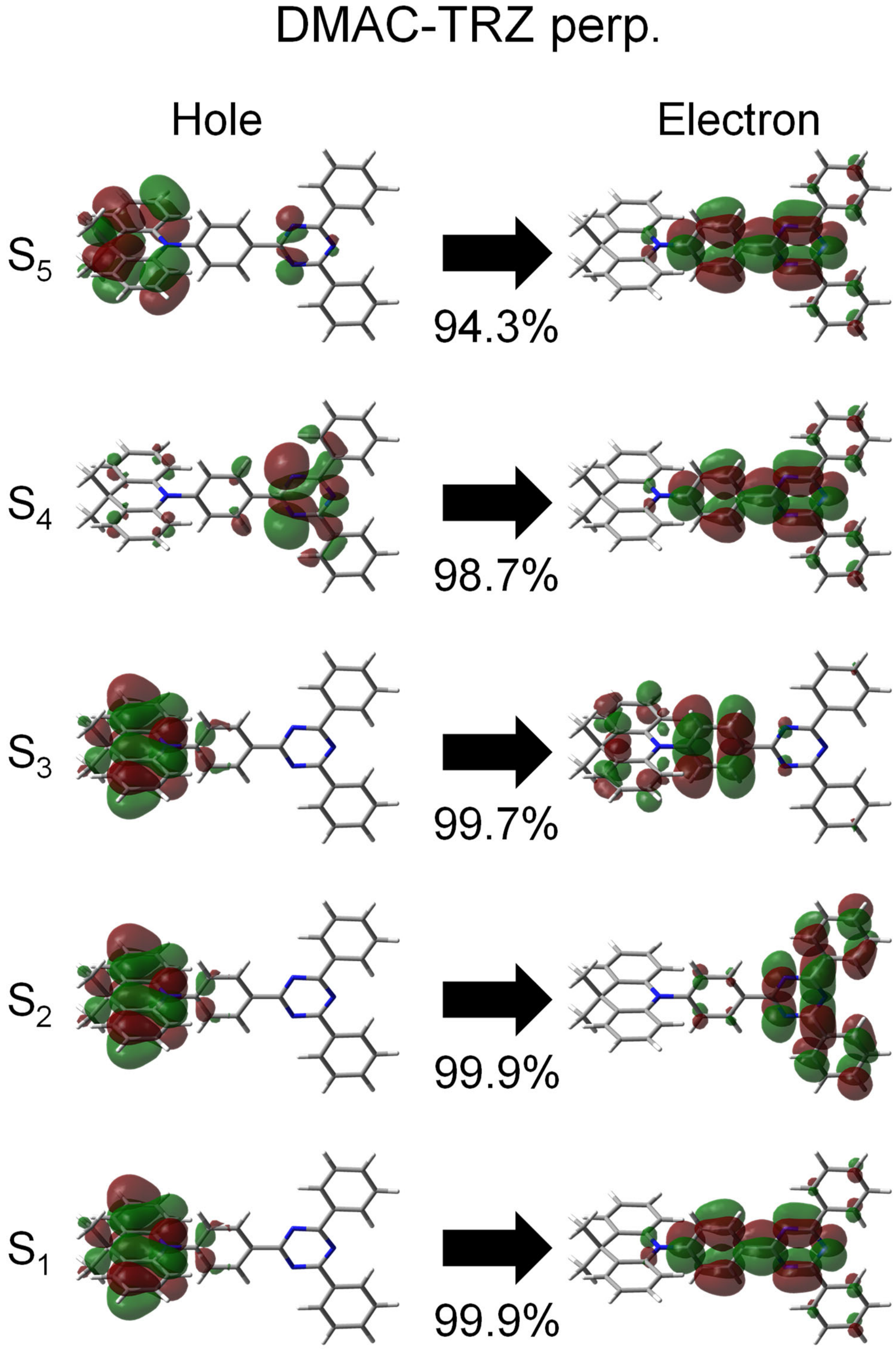

Figure S11. The NTOs of the perp. conformer of DMAC-TRZ in the S_1 to S_5 state.

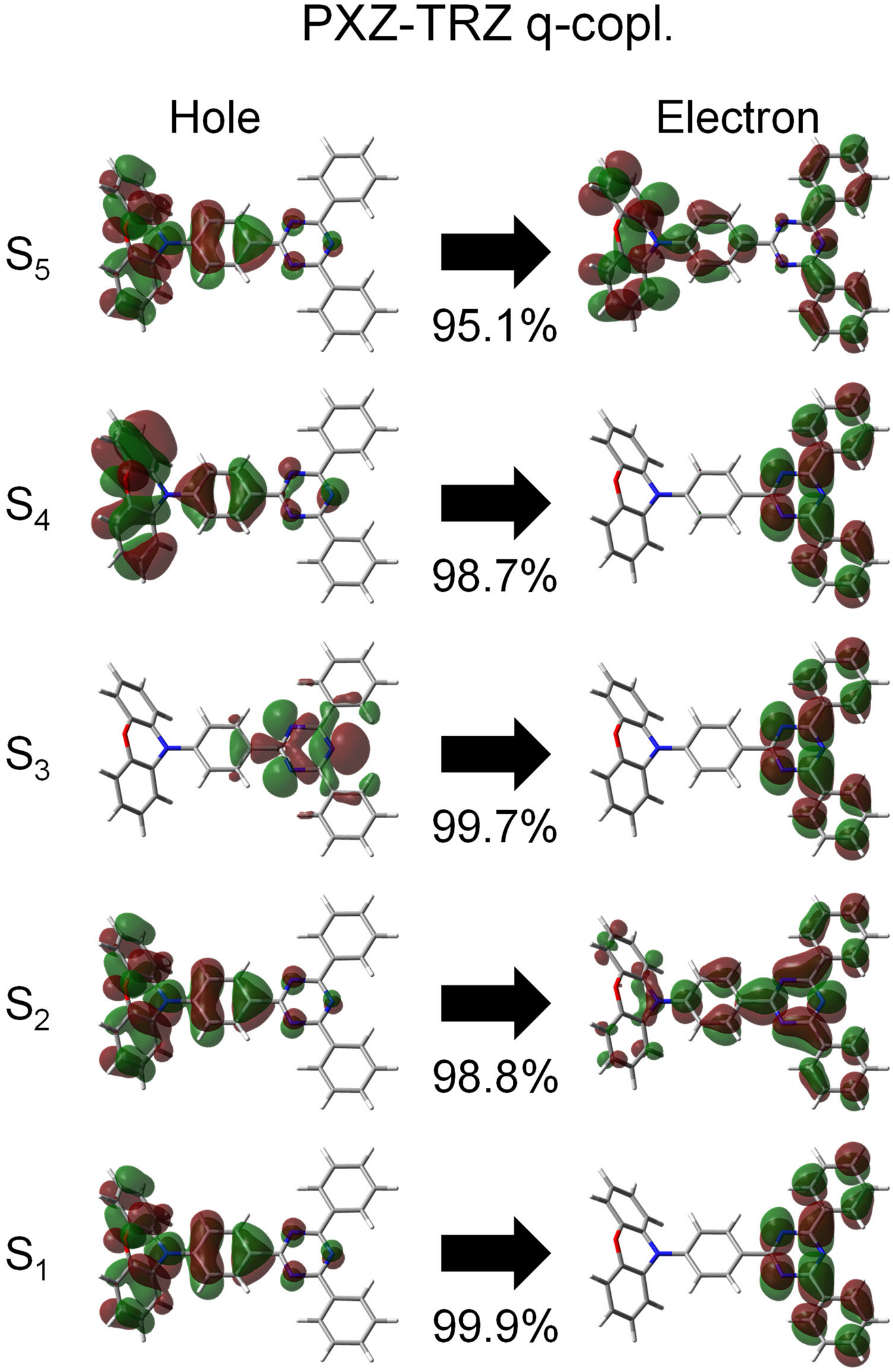

Figure S12. The NTOs of the q-copl. conformer of PXZ-TRZ in the S_1 to S_5 state.

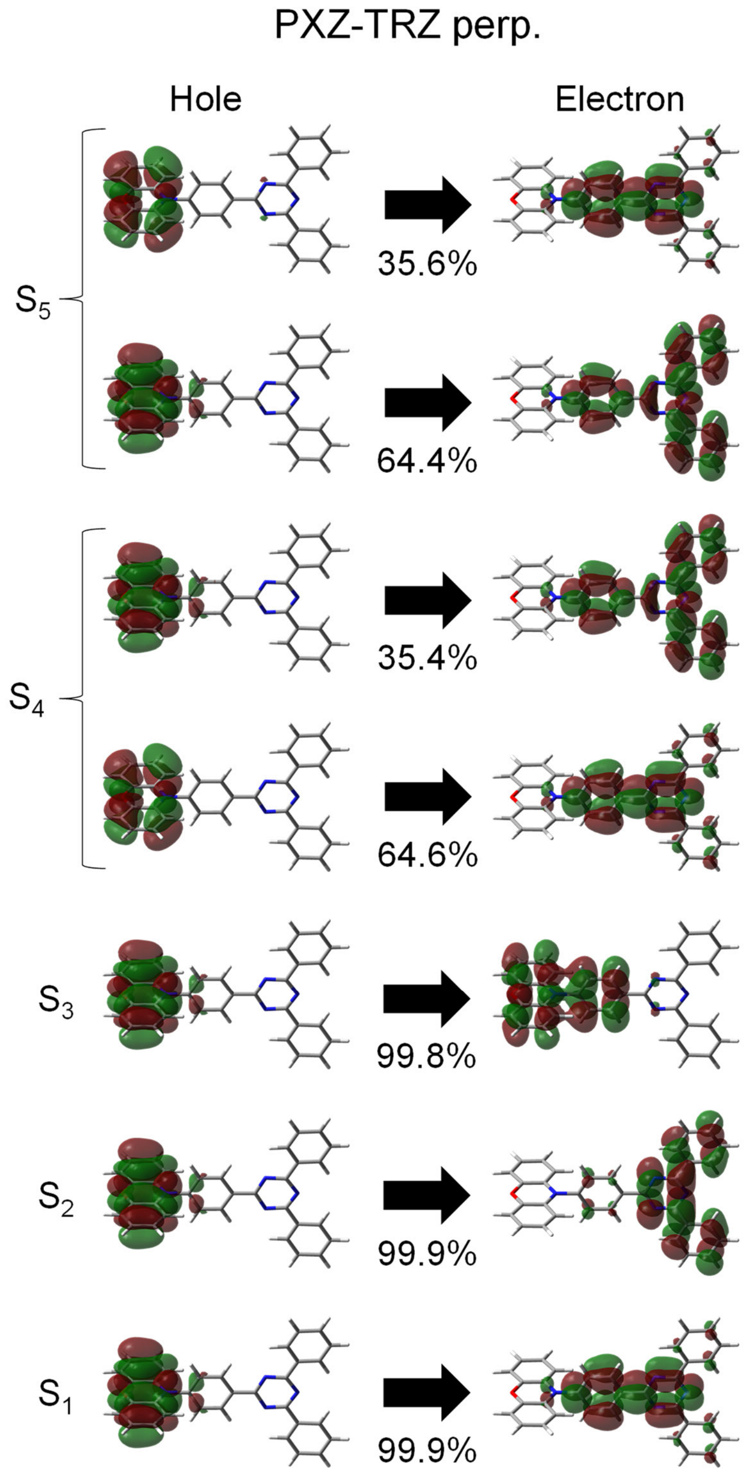

Figure S13. The NTOs of the perp. conformer of PXZ-TRZ in the S_1 to S_5 state.

SI-4. Global analysis for TR-PL spectra in toluene solution

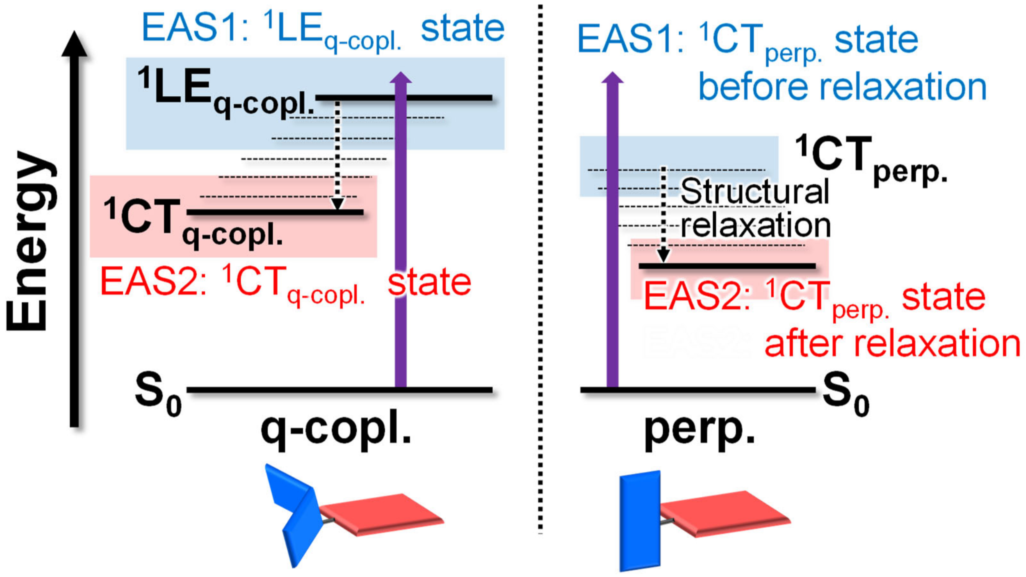

Figure S14. The model of the global analysis for the TR-PL spectra. For the q-copl. conformer, the EAS1 and EAS2 correspond to the $^1LE_{q\text{-}copl.}$ and $^1CT_{q\text{-}copl.}$, respectively. For the perp. conformer, those correspond to the $^1CT_{perp.}$ state before and after structural relaxation, respectively.

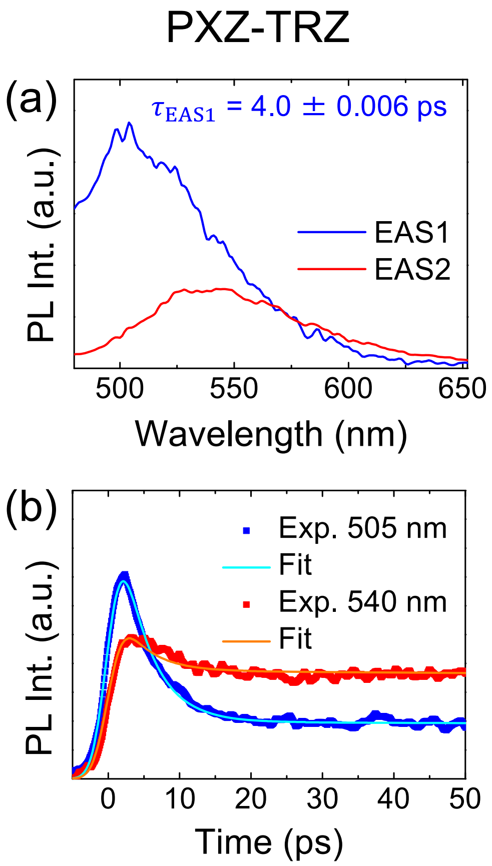

Figure S15. (a) The EAS of PXZ-TRZ derived from the TR-PL spectra of the perp. conformer using a global analysis. (b) Comparison of the time profiles of the TR-PL spectra and the fitting functions of the global analysis. The global analysis was conducted using a sequential two-state model.

Table S2. The time constants estimated by global analysis for the TR-PL spectra in toluene solution. τ_{EAS1} is the time constant of EAS1.

τ_{EAS1} (ps)	q-copl.	perp.
PTZ-TRZ	5.2 ± 0.006	-
DMAC-TRZ	6.8 ± 0.01	-
PXZ-TRZ	3.3 ± 0.008	4.0 ± 0.006

SI-5. Global analysis for TR-PL spectra in DCM solution

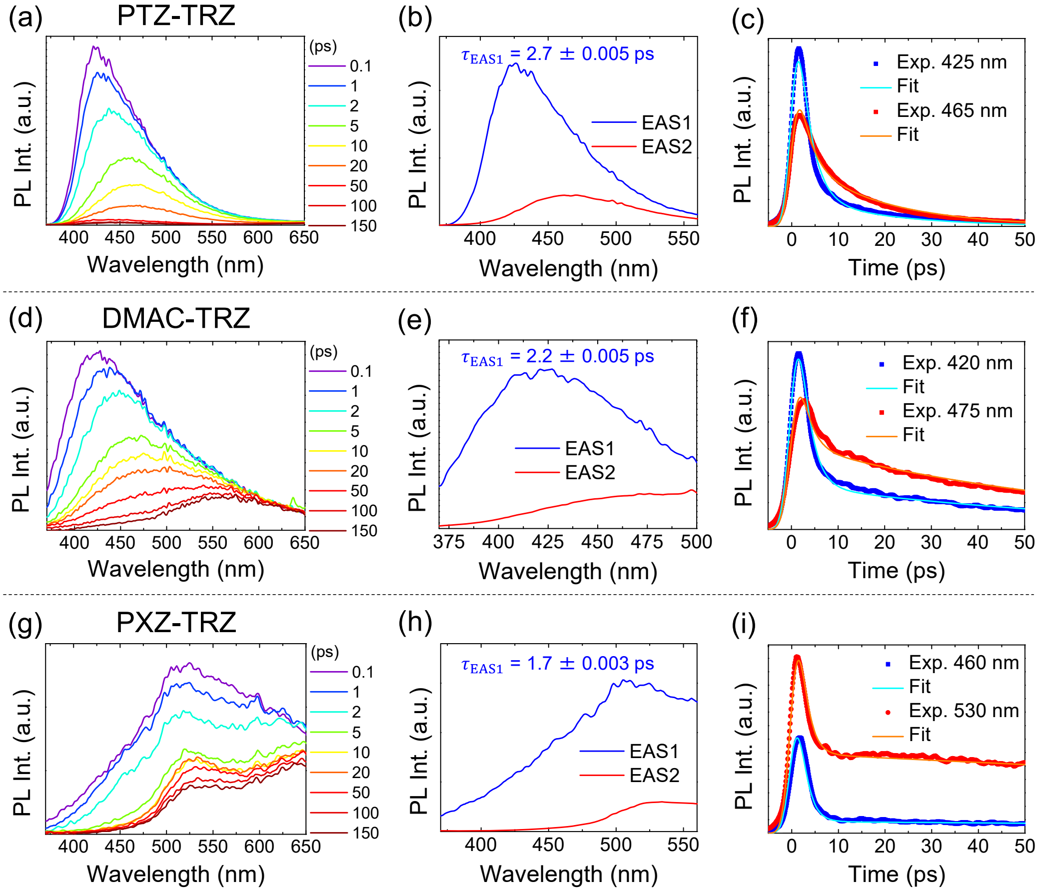

Figure S16. The TR-PL spectra of the q-copl. conformer of (a) PTZ-TRZ, (d) DMAC-TRZ, and (g) PXZ-TRZ in a DCM solution. The excitation wavelengths were 343 nm. The EAS of (b) PTZ-TRZ, (e) DMAC-TRZ, and (h) PXZ-TRZ derived from the TR-PL spectra using a global analysis. Comparison of the time profiles of the TR-PL spectra and the fitting of the global analysis for (c) PTZ-TRZ (425 and 465 nm), (f) DMAC-TRZ (420 and 475 nm), and (i) PXZ-TRZ (460 and 530 nm). The global analysis was conducted using a sequential two-state model for all the molecules.

SI-6. Functional Dependence of Ground State Energy

Table S3. Comparison of the S_0 energies of the q-copl. conformer with respect to that of the perp. conformer (ΔE in Figure 5) among B3LYP, CAM-B3LYP, and PBE0 functionals for the PTZ-TRZ and PXZ-TRZ.

	B3LYP	CAM-B3LYP	PBE0
PTZ-TRZ	-28 meV	-9.9 meV	-35 meV
PXZ-TRZ	114 meV	101 meV	98 meV

SI-7. Potential energy surface in the S_0 state

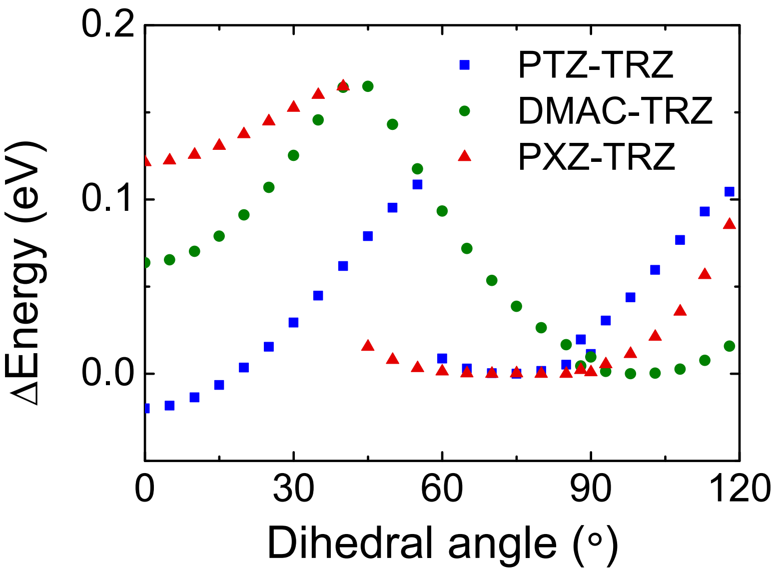

Figure S17. Calculated potential energy surfaces along the D-A dihedral rotation of the three molecules in the S_0 state. The structure with the dihedral angle of 0° and 90° are assigned to the q-copl. and perp. conformer.

Table S4. Calculated activation energy from 0° to 90° and from 90° to 0°. E_a is the activation energy for each direction.

	E_a (0° → 90°)	E_a (90° →0°)
PTZ-TRZ	128 meV	109 meV
DMAC-TRZ	101 meV	165 meV
PXZ-TRZ	44 meV	165 meV

SI-8. Stereo-structural factors contributing to the stability of the q-copl. conformer

The stability of the q-copl. conformer varies among the molecules, with the order of stability being PTZ-TRZ < DMAC-TRZ < PXZ-TRZ. We discuss this difference in terms of the molecular stereo-structure based on the DFT calculations. The structures for all the three molecules were optimized in the S_0 state. The solvent effect was examined by using the polarizable continuum model of toluene solution. We employed the 6-31G(d,p) basis set and B3LYP functional. The existence of the q-copl. conformer in these molecules is attributed to the folding angle of the donor plane and the bending angle of the donor relative to the acceptor. To quantify these structural features, we defined the folding angle of the donor plane as θ_{Fold} and the bending angle of the donor as θ_{Bent} (Figures S18a,b), and compared these angles across the three molecules (Figures S18c). Regarding θ_{Fold}, PTZ-TRZ and DMAC-TRZ exhibited significant folding, while for θ_{Bent}, PTZ-TRZ and PXZ-TRZ showed more pronounced bending. The magnitude of θ_{Fold} is likely caused by repulsion between the lone pairs on heteroatoms or by steric hindrance from the dimethyl groups in the donor plane. The relatively small θ_{Bent} in DMAC-TRZ can be due to electron repulsion between the dimethyl group in DMAC and TRZ. These electronic factors may determine the stability of the q-copl. conformer. Therefore, the simultaneous occurrence of strong repulsion between lone pairs in sulfur and low electronic repulsion between the donor and acceptor moieties in PTZ-TRZ is suggested to contribute to the stability of the q-copl. conformer. Furthermore, a comparison between DMAC-TRZ and PXZ-TRZ suggests that electronic repulsion between lone pairs in donor contributes more significantly to the stabilization of energy of the q-copl. conformer than electronic repulsion between the donor and acceptor moieties. These findings elucidate the relationship between the stereo-structure and the stability of the q-copl. conformer.

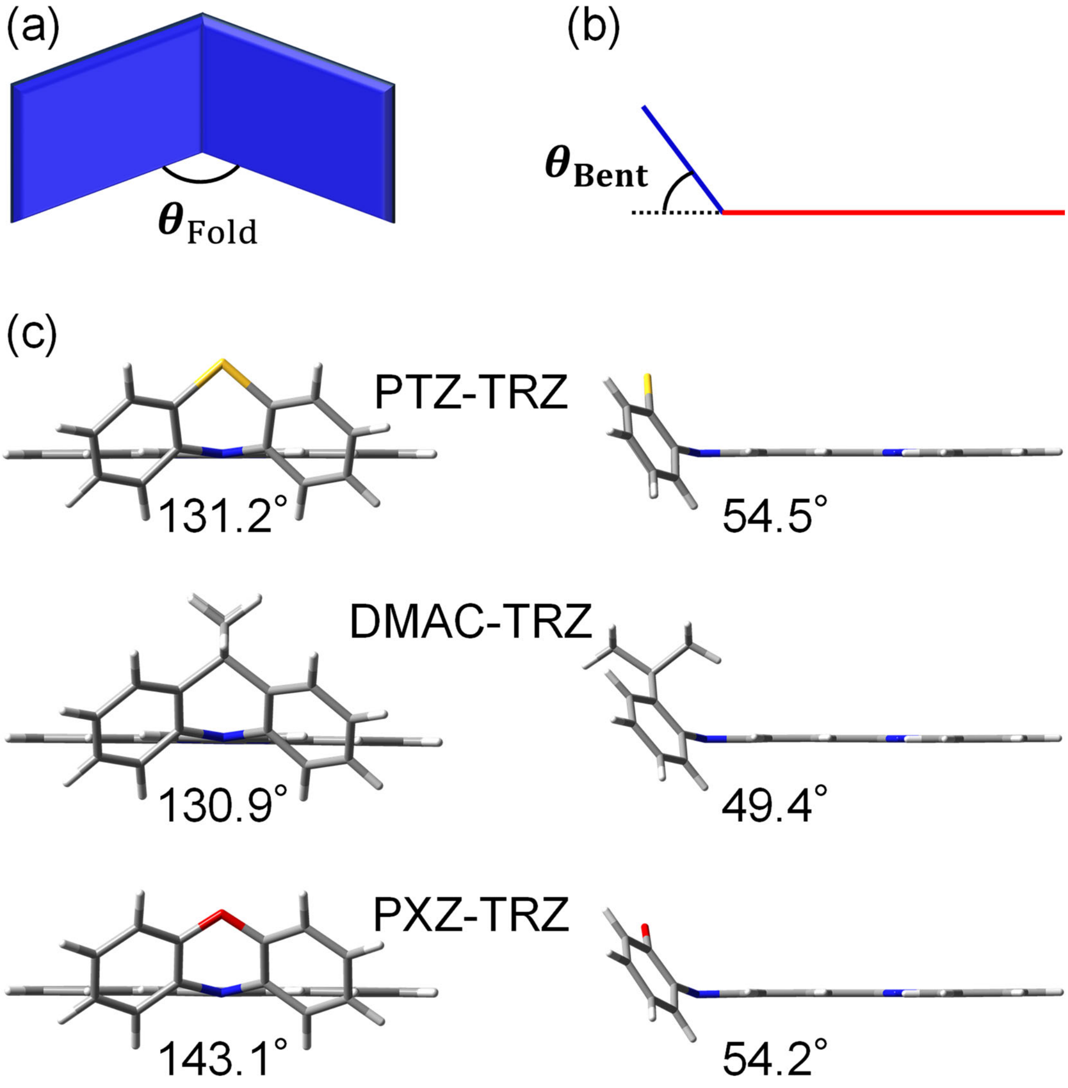

Figure S18. Scheme of (a) θ_{Fold} and (b) θ_{Bent}. (c) Stereo-structure of the PTZ-TRZ, DMAC-TRZ, and PXZ-TRZ in the S_0 state, and θ_{Fold} and θ_{Bent} of each molecule.

SI-9. Correlation between $I_{\mathrm{E,q-copl.}}/I_{\mathrm{E,perp.}}$ and $N_{\mathrm{q-copl.}}/N_{\mathrm{perp.}}$

We discuss the correlation between $I_{\mathrm{E,q-copl.}}/I_{\mathrm{E,perp.}}$ and $N_{\mathrm{q-copl.}}/N_{\mathrm{perp.}}$. In general, emission intensity (I_{E}) is proportional to the following equation:

$$I_{\mathrm{E}} \propto \varepsilon \times N \times \phi_{\mathrm{PL}} \tag{S2}$$

where ε is the molar absorption coefficient at the excitation wavelength, N is the population in the ground state, and ϕ_{PL} is the photoluminescence quantum yield. Here, $I_{\mathrm{E,q-copl.}}$ and $I_{\mathrm{E,perp.}}$ represent the intensity of the emission from the $^1\mathrm{LE}_{\text{q-copl.}}$ state and that from the $^1\mathrm{CT}_{\text{perp.}}$ state before structural relaxation, respectively. Since these emissions originate from the excited states immediately after photoexcitation, where the effects of relaxation are negligible, ϕ_{PL} can be regarded as unity. Because the absorption spectra in Figure 1 show mixture absorption of the two structures at the excitation wavelength, 343 nm, it difficult to determine ε of each structure at 343 nm. However, in crude approximation ε is regarded to be proportional to the oscillator strength; thus, the ratio of the oscillator strength of the two conformer $f_{\mathrm{q-copl.}}/f_{\mathrm{perp.}}$, can be estimated by dividing $I_{\mathrm{E,q-copl.}}/I_{\mathrm{E,perp.}}$ by $N_{\mathrm{q-copl.}}/N_{\mathrm{perp.}}$. The estimated $f_{\mathrm{q-copl.}}/f_{\mathrm{perp.}}$ were 47.9 for PTZ-TRZ, 164 for DMAC-TRZ, and 123 for PXZ-TRZ, respectively, indicating that the oscillator strengths for all the molecules are similar at least the same order. This result is consistent with those by the quantum chemical calculations shown in Table S1, that is, the oscillator strengths of the $^1\mathrm{LE}_{\text{q-copl.}}$ state (S_2 state) and the $^1\mathrm{CT}_{\text{perp.}}$ state (S_1 state) do not significantly depend on the molecule. Thus, it is reasonable that the difference in the population in the S_0 state between the conformers determines the emission intensity ratio between the conformers immediately after photoexcitation.

SI-10. Normalized TA spectra

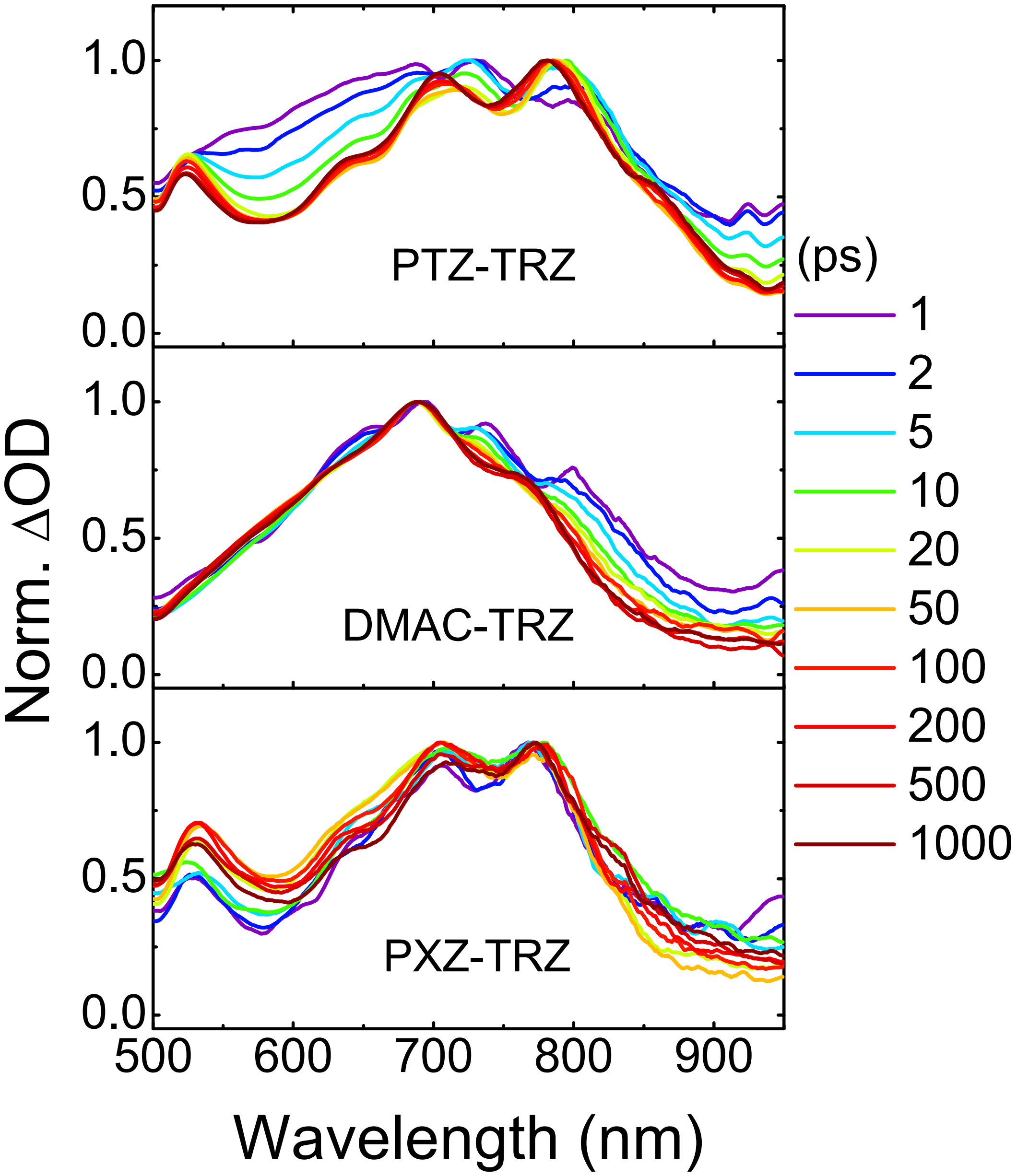

Figure S19. The normalized TA spectra in PTZ-TRZ, DMAC-TRZ, and PXZ-TRZ

SI-11. Global analysis for TA spectra

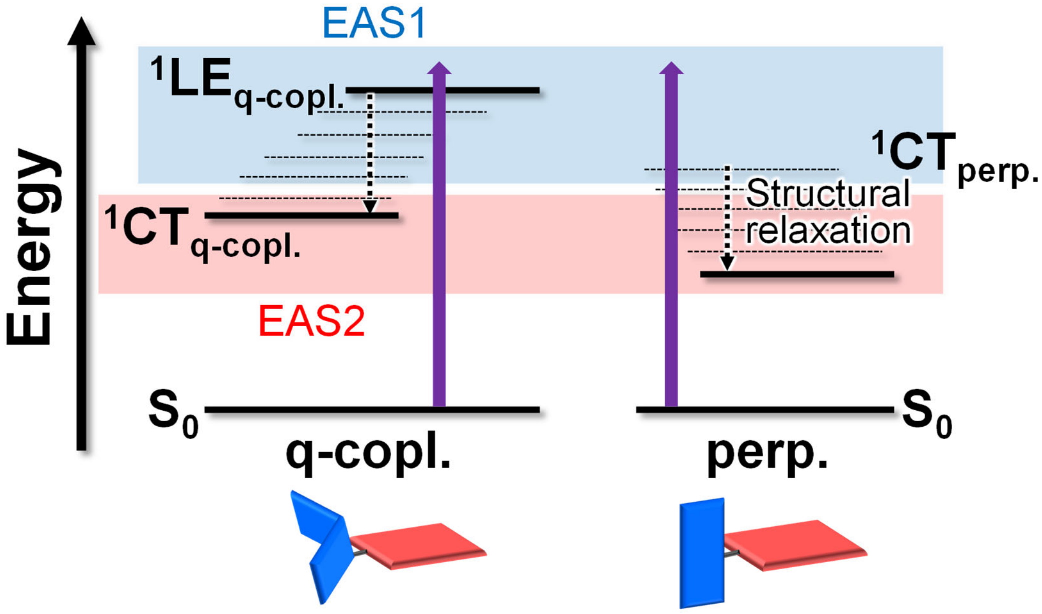

Figure S20. The model of the global analysis for the TA spectra. EAS1 and EAS2 correspond to the coexistence states of the ^{1}LE$_{q\text{-copl.}}$ state and the ^{1}CT$_{perp.}$ state before structural relaxation, and the coexistence states of the ^{1}CT $_{q\text{-copl.}}$ state and the ^{1}CT$_{perp.}$ state after the relaxation, respectively.

Reference

(1) Frisch, M. J.; Trucks, G. W.; Schlegel, H. B.; Scuseria, G. E.; Robb, M. A.; Cheeseman, J. R.; Scalmani, G.; Barone, V.; Petersson, G. A.; Nakatsuji, H.; Others. Gaussian 16, Revision C.01. **2016**, Gaussian Inc., Wallingford CT.